ISSN 1061-9348, Journal of Analytical Chemistry, 2023, Vol. 78, No. 10, pp. 1281–1294. © The Author(s), 2023. This article is an open access publication, corrected publication 2023.
Russian Text © The Author(s), 2023, published in Zhurnal Analiticheskoi Khimii, 2023, Vol. 78, No. 10, pp. 867–882.

REVIEWS

Tunable Diode Lasers for Analytics and Diagnostics

M. A. Bolshov[a], *, **, Yu. A. Kuritsyn[a], V. V. Liger[a], V. R. Mironenko[a], and Ya. Ya. Ponurovskii[b]

[a] *Institute of Spectroscopy, Russian Academy of Sciences, Troitsk, Moscow, 108840 Russia*
[b] *Prokhorov General Physics Institute, Russian Academy of Sciences, Moscow, 119991 Russia*
**e-mail: mbolshov@mail.ru*
***e-mail: bolshov@isan.troitsk.ru*

Received May 23, 2023; revised June 6, 2023; accepted June 7, 2023

Abstract—Continuous-wave diode lasers (DLs) with tunable emission wavelengths have become extensively used in various fields of analytical spectroscopy and diagnostics. Working in the near and mid-IR spectral region, tunable diode lasers are particularly effective in detecting simple molecules, making them invaluable for environmental monitoring, industrial process control, and diagnostics of subsonic and supersonic gas flows. However, the lack of commercial diode lasers operating in the spectral region shorter than 400 nm has restricted their applicability to elemental analysis, as many resonance lines of free atoms of elements lie in the region 250–400 nm. This review aims to highlight various applications of continuous diode lasers, which are lesser-known to analytical chemists. We briefly overview their main characteristics and discuss their advantages, enabling their successful implementation in traditional analytical spectroscopy tasks, as well as for diagnosing parameters of remote gas objects, including combustion processes in mixing gas flows.

Keywords: diode lasers, absorption spectroscopy, gas analysis, diagnostics of hot zones
DOI: 10.1134/S1061934823100052

Continuous-wave diode lasers (DLs) with tunable emission wavelengths have found wide applications to various fields of analytical spectroscopy and diagnostics [1–12]. These instruments have several unique characteristics, which ensured their diverse applications to both the local and remote determination of analytes and/or parameters of probed media:

(1) Commercially available distributed-feedback diode lasers (DFB-DLs) operate in a single-mode at room temperature in the spectral region from ~760 nm to 3 μm;

(2) Single-mode diode lasers have a narrow spectral emission widths ($<10^{-3}$ cm^{-1} or $<10^{-4}$ nm in the spectral region of 1 μm), which is much narrower than the typical absorption linewidths of free atoms and molecules (~0.05 nm). Such a small spectral width of a diode laser line eliminates the need in using bulky and expensive optical spectrometers for the spectral selection of a useful analytical signal;

(3) The diode laser radiation wavelength can be tuned rapidly over a time of about 1 μs in the region 0.1–0.3 nm due to a change in the injection current or more slowly over a time of an order of a second in the region of 1–1.5 nm due to a change in the temperature of the laser chip;

(4) The power of a diode laser used in analytics can vary within 1–50 mW. Such power is sufficient for the detection of a signal that has passed through a studied gaseous medium even at long optical path lengths and significant nonselective absorption;

(5) The diode laser radiation can be easily collimated by a simple optical system and delivered to a sufficiently remote object. The radiation emerging from the laser chip is efficiently coupled into a single-mode fiber and can be delivered losslessly over long distances;

(6) Diode lasers are rather compact, and sensors based on them possess small dimensions and weights;

(7) Diode lasers of the simplest designs are relatively cheap, which ensures acceptable prices for respective spectrometers.

The dependences of the radiation power and wavelength on the injection current for a typical single-mode diode laser are shown in Fig. 1. With arising injection current through the laser chip, the power grows, and the radiation wavelength increases. Unfortunately, the tuning characteristic of the majority of DFB-DLs, i.e., the dependence of the radiation frequency on current, is nonlinear, creating certain problems in processing the measurement results.

This review gives examples of the use of diode lasers in various areas of analytical spectroscopy for determining the concentration of atomic or molecular components in samples in different aggregate states and for determining the parameters of hot zones (temperature, partial and total pressure of gas mixtures).

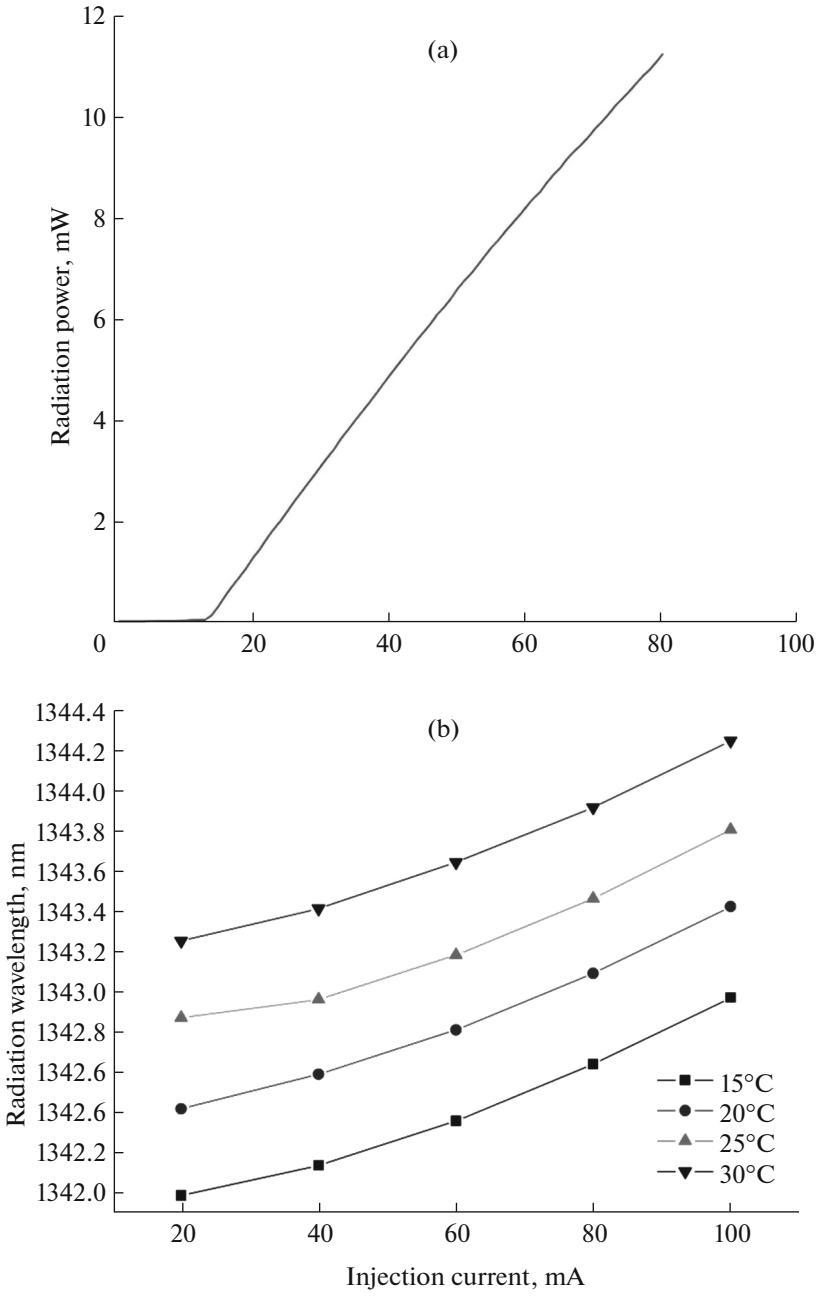

Fig. 1. Dependences of (a) the radiation power of a typical laser with distributed feedback and (b) radiation wavelength on the injection current.

EXAMPLES OF APPLICATIONS OF DIODE LASERS

Combined method for determining uranium isotopes. The determination of ^{235}U and ^{238}U uranium isotopes is the crucial task of analytical control in the production of nuclear materials and in the processing of nuclear wastes. This problem is usually solved by rather expensive methods of inductively coupled plasma–mass spectrometry (ICP–MS), thermal ionization mass spectrometry (TIMS), or neutron activation analysis. A combination of the laser evaporation of a solid material (laser ablation) and laser-induced fluorescence (LIF) [13] or atomic absorption spectrometry (AAS) [14] with the use of tunable DL radiation turned out to be a promising method for determining the rare ^{235}U isotope against the background of the abundant ^{238}U isotope. In [13, 14], the minor isotope of uranium was determined in a solid sample against the background of the dominant content of the main ^{238}U isotope. The samples were three com-

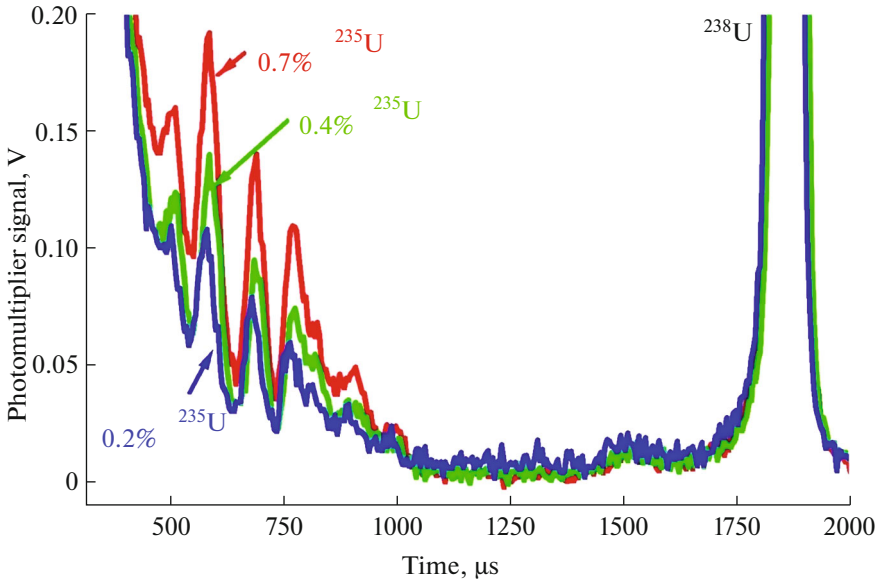

Fig. 2. Fluorescence spectra of three uranium samples with ^{235}U concentrations of 0.2, 0.4, and 0.7%. The start of recording the spectra coincides with the pulse of the evaporating laser. The fluorescence of the main ^{238}U isotope is recorded approximately 750 μs after the start of recording, when the concentration of the evaporated material in the probing zone has significantly decreased [13].

pressed tablets of graphite uniformly mixed with uranium oxide containing the ^{235}U isotope: 0.714% (natural abundance of the isotope), 0.204, and 0.407% (uranium oxide depleted in ^{235}U).

The radiation of a pulsed neodymium glass solid-state laser was focused on the surface of a solid sample, and the region of the plasma of the evaporated material was illuminated by the frequency-tunable diode laser radiation. The largest isotopic shift for the ^{235}U and ^{238}U isotopes was observed for the atomic lines at 682.6913 (^{238}U) and 682.6736 nm (^{235}U) lines; it was $\Delta\nu^{238-235} = -0.3798$ cm^{-1} ($\Delta\lambda = 17.7$ pm). In the experiment, the diode laser was turned on at the moment of the generation of a short evaporating pulse of the solid-state laser, and the DL frequency was scanned in the region of the isotope absorption lines.

Transmitted DL radiation (AAS) or laser-induced fluorescence (LIF) of free uranium atoms was recorded only for a time interval, the duration and beginning of which were selected according to the maximum signal-to-noise value. During laser ablation, a plasma bunch of the evaporated material formed above the target surface, and this plasma scattered from the surface, significantly decreasing the concentration of the evaporated material with time. The continuous background determined by the plasma radiation also decreased with time, resulting in a space–time window during which the signal-to-noise ratio was maximum. An example of recording the fluorescence spectra of uranium isotopes for the three samples with different concentrations of the minor isotope is shown in Fig. 2. The narrow DL radiation line allowed for the filtering of the analytical signal without an optical monochromator. The figure shows the hyperfine structure of the fluorescence radiation, which can be resolved by optical spectroscopy only with powerful and expensive triple monochromators. The limits of detection were 0.6 (LIF) and 0.1 mg/g (AAS).

Determination of gas flow rate. Gas flow rate is an essential parameter in the diagnosis of various processes in flows. The simplest method for measuring the flow rate is to measure the Doppler shift of the absorption line maximum of a certain test molecule. Narrow-band diode lasers ensure both sufficient simplicity and accuracy of flow rate measurements. The DL radiation is divided into two beams that cross the flow in opposite directions at a certain angle of θ. The maxima of the absorption line of the test molecule are determined when the flow is probed at an angle of 90° to the direction of the flow and at angles ±θ to the direction of the flow. The shift of the absorption line maxima during flow probing at the angles ±θ is $\Delta\nu_D = 2V/c\nu_0\sin\theta$, where V is flow rate, c is speed of light, and ν_0 is absorption line maximum during normal flow probing. Using two probing directions of ±θ doubles the difference in the measured shifts, i.e., increases the accuracy of the rate measurement. For the near-IR diode lasers, the Doppler shift is approximately 3×10^{-5} cm^{-1} per 1 m/s. The accuracy of the flow rate determination and the features of such an estimate for a nonuniform flow were discussed in [15].

DIODE LASER ABSORPTION SPECTROSCOPY

Diode laser absorption spectroscopy (DLAS) is the most widely used method.

Elemental analysis. In the 1980–1990s, methods were developed for determining small concentrations of elements by DLAS using flame or graphite atomizers [16]. The first experiments on the determination of alkali metals were quite successful. The limits of detection for analytes by DLAS were significantly lowered in comparison with those in AAS using conventional sources of resonance radiation, such as hollow cathode lamps. However, the vulnerable spot of DLAS was the lack of diode lasers emitting in the UV spectral region shorter than 400 nm, where strong resonance lines of the vast majority of elements lie. Therefore, DLAS turned out to be unsuitable for elemental analysis.

Molecular spectrometry. The DLAS method has become the most popular for determining the concentration of molecules in various gas mixtures and for the remote determination of the parameters of hot zones and processes occurring in them.

In DLAS, the probing DL radiation passes through a gas object under study, and the recording system measures the intensity of the transmitted radiation. The DL wavelength is tuned within the selected spectral region, and when it coincides with the absorption line of the test molecule, a decrease in the intensity of the transmitted DL radiation is recorded. If the absorption line is strong enough ($\Delta I/I_0 \geq 10^{-3}$), this dip can be directly detected. To detect weak lines, modulation versions of DLAS have been developed, which are discussed below.

HOT ZONE MEASUREMENTS

Direct absorption measurement mode. DLAS is widely used to diagnose the parameters of hot zones, in particular, for remote diagnostics of combustion processes in mixed flows of a fuel (hydrogen, hydrocarbons) and an oxidizer (oxygen, air) [5–8]. The main constantly monitored parameters are temperature, concentration of the main molecular components of the mixture, and total pressure in the combustion zone. The key advantage of DLAS as a method of diagnostics is its remote character, because any measuring device, such as a thermocouple introduced into the flow distorts the thermal and hydrodynamic field around such an object, significantly distorting the measurement results. The DL probing beam does not affect the spatial or time distribution of the thermal and acoustic fields in the probed area and ensures the correct determination of the required parameters of the medium.

The DLAS measurement of the temperature of a gaseous medium is based on an assumption of a thermodynamic equilibrium (TDE) in the combustion zone. This assumption is valid for the characteristic times of the processes of about several submilliseconds and at a total pressure of the gas mixture higher than 0.1 atm. By tuning the wavelength of the DL radiation, one can record the intensities of different absorption lines and determine temperature from their ratio. When the TDE condition is satisfied, the distribution of molecules over energy levels obeys the Boltzmann law, and the ratio R of the integral intensities of two absorption lines of the test molecule with different lower levels $E_{1,2}$ obeys the equation

$$R = \left(\frac{S_1}{S_2}\right)_{T_0} \exp\left[-\frac{hc\Delta E}{k}\left(\frac{1}{T} - \frac{1}{T_0}\right)\right],$$

where $S_{1,2}$ are line intensities for temperature T_0; ΔE is energy difference of the lower levels; T is temperature; and h, c, and k are universal constants.

Typical parameters of combustion zones in the gas flows are the following: size of the test zone is 70–150 mm, total pressure of the mixture is 0.1–3 atm, temperature is up to 3000 K, the duration of the combustion process is 0.1–10 s, fuel is hydrogen or hydrocarbons, and flow rates are up to M ~ 2–3 (M is the Mach number). The majority of the works with DFB-DLs were devoted to the detection of water molecules, which is a product of the combustion reaction of hydrocarbons. The concentration of water molecules at the last stages of the process determines the efficiency of the fuel use.

The optimal circuits including the DLAS technique were selected depending on the specific conditions of the combustion process. A series of studies [17–19] performed with colleagues from the Joint Institute for High Temperatures of the Russian Academy of Sciences examined hydrogen or ethylene combustion under a static pressure of ~150 Torr and a flow rate of M = 2. Under these conditions, the absorption lines of water are rather narrow, and we found a spectral region where three lines overlapped only slightly with their wings. These lines have different lower energy levels, and the population of these levels and the intensity of the lines depend on the temperature of the mixture. Using spectroscopic databases [20], we calculated the intensities of the selected lines for different temperatures. The calculation results (Fig. 3) show a strong change in the line intensity ratios for different temperatures.

The experiments were carried out using an experimental stand at the Joint Institute for High Temperatures of the Russian Academy of Sciences. The design of the stand included an optical block with pairs of windows for the input and output of a probing DL beam, crossing the gas flow in a perpendicular direction. Various sections of the combustion zone were probed. Combustion in the mixing flows of hydrogen and air was initiated and maintained by an electric discharge. One run of the setup lasted 0.5 s; the discharge was switched on after the flow reached the quasi-steady-state conditions and was maintained for 80–

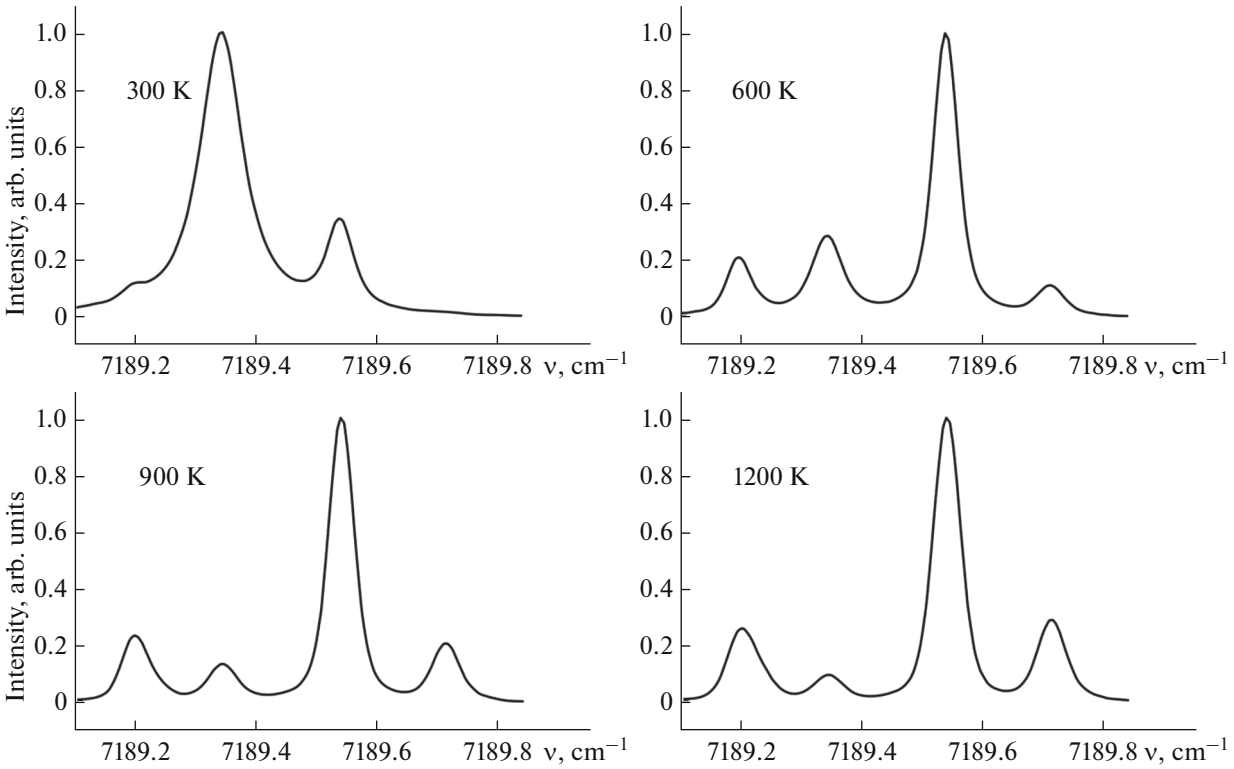

Fig. 3. Spectra of a water molecule calculated for different temperatures based on spectroscopic databases.

100 ms. Fuel injection was switched 20–30 ms after the start of the discharge and switched off 20–30 ms after the discharge was terminated. The combustion stopped at the moment the discharge was turned off.

In the study of nonsteady-state processes, the fast tuning of the DL wavelength made it possible to scan repeatedly the gas object under study. The DL wavelength could be scanned over the entire tuning range in ~1 ms. During the time of the development of a nonsteady-state process of ~1 s, the object of interest could be probed 10^3 times. However, essential events developed only at a certain time interval of the entire process.

A method for the primary processing of a data array, developed in [17], helped to detect the most important and interesting stages of the studied nonsteady-state process. The recorded spectra were initially processed by converting the raw scans into a two-dimensional image. This procedure greatly simplified the initial general overview of the recorded run and highlighted the time stages in the development of the combustion process.

An example of recording one run is shown in Fig. 4. The experimental results obtained in one run are a data array, consisting of 2×10^6 points. The array contains a record of ~600 scans of the DL wavelength tuning in the selected spectral region. In each scan, injection current is changed according to a sawtooth law, with current increasing linearly in the first half of the scan and decreasing linearly in the second half. The total recording time is 500 ms. The working parameters in this run were as follows: static pressure in the test section, 130 Torr; hydrogen flow rate, 0.5 g/s. Figure 4 presents the constructed two-dimensional image of the process (Fig. 4a) and absorption spectra near 7189 cm^{-1}, obtained by averaging over 60 adjacent scans (Fig. 4b). In the time interval indicated in part I, there is air in the chamber at a pressure of ~120 Torr. Both the 2D image and the spectrum corresponding to this time interval show the "cold" line at 7189.344 cm^{-1} (line *1*). At the end of interval I, the flow in the channel reaches the supersonic mode; the static gas temperature here is $T \approx 200$ K, i.e., well below room temperature. This causes water vapor to freeze, leading to the disappearance of water absorption lines within 20–30 ms, as observed in the two-dimensional image and the corresponding spectrum during time interval II. At a time of ~120 ms from the start, the discharge is switched on, and fuel injection begins approximately 20 ms later. The combustion process is initiated at this moment, accompanied by a rapid rise in temperature and the appearance of water vapor in the combustion zone. The figure shows high-lying H_2O absorption lines: 7189.715, 7189.541, and 7189.199 cm^{-1} (lines *2*, *3* and a weak line that was not involved in the processing of the results). At the same time, the low-lying "cold" line at 7189.344 cm^{-1} noticeably weakened. This character of the spectrum

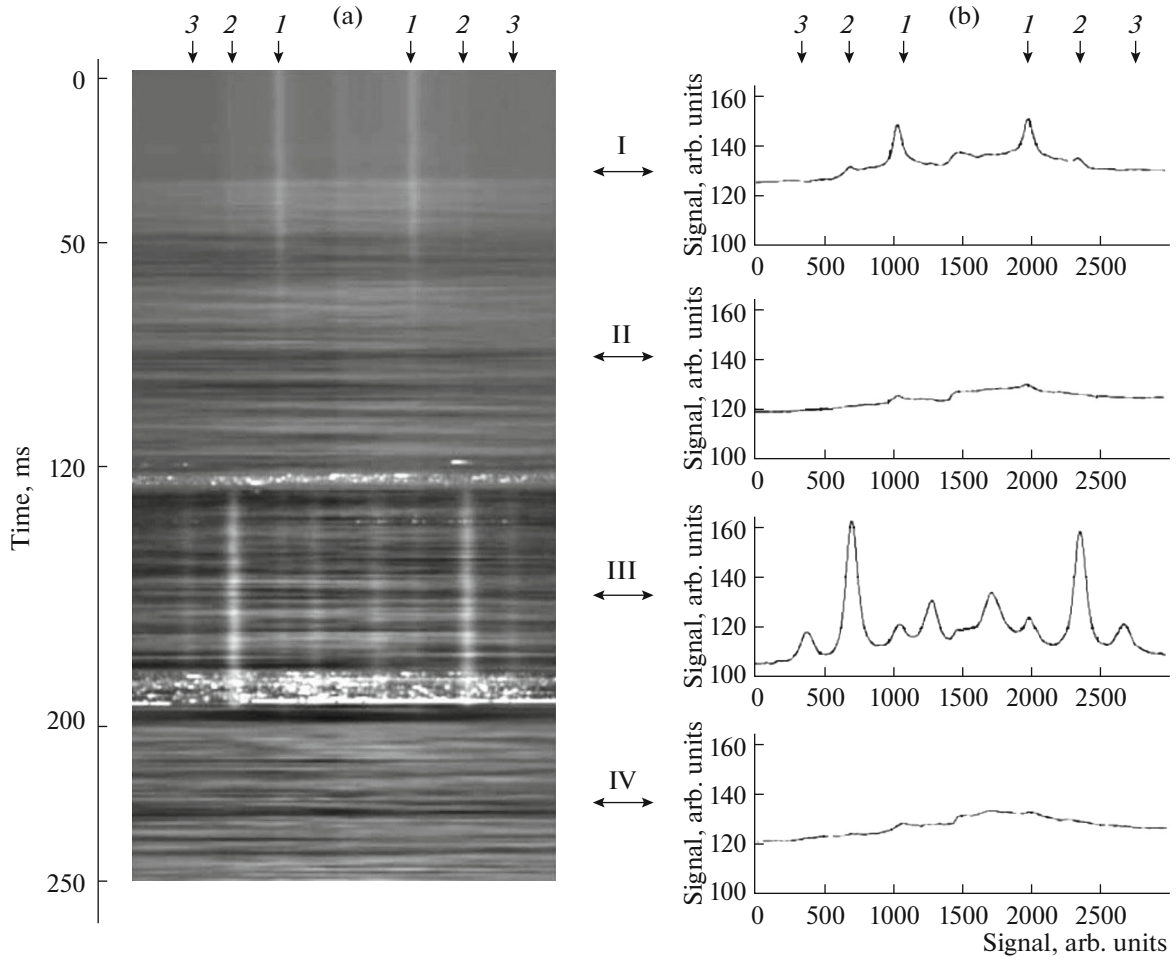

Fig. 4. Processing a data array obtained by recording one run of a power device at the Joint Institute for High Temperatures, Russian Academy of Sciences [17]: (a) a 2D image of all scans acquired in the first 250 ms and (b) the H_2O absorption spectra averaged over 60 scans in different intervals of the development of the combustion process. (I)–(IV) Positions of the absorption line maxima used for subsequent processing. Identification of lines at (*1*) 7189.344, (*2*) 7189.541, and (*3*) 7189.714 cm^{-1}.

remained unchanged over the entire time interval III of approximately 50 ms, when the combustion process was maintained. In the end of this interval, the combustion process stopped (Fig. 4, part IV), and the temperature of the supersonic flow dropped rapidly, which led to the freezing of water vapor and the disappearance of almost all water absorption lines. This is seen in the left panel after approximately 200 ms.

For the run shown in Fig. 4, the average temperature of the probed zone over the indicated time interval and the partial pressure of water recalculated from the concentration of molecules were 1050 K and 21 Torr, respectively. The value of the total pressure of the mixture in the probed zone, $P = 200$ Torr, agrees well with the results of independent measurements by static pressure sensors.

The problem solved in collaboration with colleagues from the Zhukovsky Central Aerohydrodynamic Institute was even more challenging. It was required to determine the temperature of a gas mixture flow in the combustion zone in the test stand chamber. The pressure in the flow could be varies up to 3 atm, and the temperature varied within 300–2000 K. Under these conditions, the absorption lines broadened to values of ~0.2–0.5 cm^{-1}, which excluded a possibility of finding a spectral region of ~1–3 cm^{-1} with nonoverlapping absorption lines. The DLAS circuit, which used one diode laser to detect multiple lines in one tuning cycle, failed to operate in such a scenario. An alternative solution was to use two diode lasers operating in different spectral regions. Such a solution enabled selecting strong absorption lines so that each laser recorded one broadened and, preferably, isolated molecular line.

The new DLAS design was installed in the T-131 test stand at the Zhukovsky Central Aerohydrodynamic Institute [21, 22]. Two diode lasers were used, operating near 1.392 μm ($\nu_1 = 7185$ cm^{-1}) and 1.343 μm ($\nu_2 = 7444$ cm^{-1}). During one run, a hot air flow was first switched on at a reduced pressure; then,

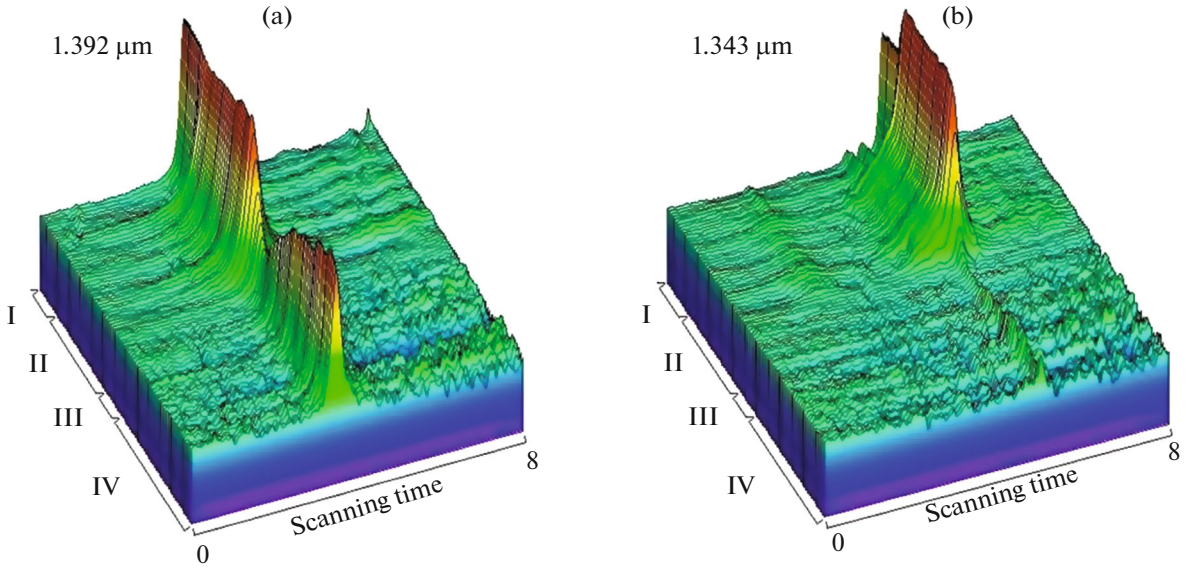

Fig. 5. 3D images of absorption spectra obtained during one run of the T-131 power unit at the Zhukovsky Central Aerohydrodynamic Institute [21] (see text for explanations).

at a certain moment, the flow was throttled by a damper, pressure and temperature increased, and, after a certain time, the throttle opened and the flow cooled. An example of recording one such run is shown in Fig. 5. The data array was primarily processed according to the method described above. Figure 5 shows the dynamics of the process: (I) the initial stage, at which the line intensities corresponded to the temperature of hot air (~700 K) at reduced pressure; (II) the stage with throttling, at which the temperature increased, the lines broadened due to an increase in pressure, while the intensity of the "hot" line (1.343 μm) increased; (III) the stage where the throttle and the air heater were switched off; (IV) the run was completed, cold blowing was switched on, the air in the chamber cooled down, and the temperature dropped to ~400 K. The "hot" line practically disappeared at the final stage, and the intensity of the "cold" one was restored.

Tomographic diode laser absorption spectroscopy. So far we considered options for using the DLAS method for diagnosing gas objects based on probing an object with a single laser beam of a diameter of about 1 mm. In this case, the parameters of the object under study were determined along one selected direction. The test gas object usually had an extended size in three dimensions, for example, the combustion zone and the exhaust gas zone in large aircraft engines, hot zones of thermal turbines, etc. We could obtain complete information about such objects only by moving the probe beam of the diode laser in two dimensions, which complicated and increased the duration of the diagnostic process. Obtaining a complete picture of the parameters of stationary processes was possible, albeit time-consuming. The issue is rather acute in the case of diagnosing short, single processes, especially when the conditions in the hot zone are irreproducible.

For such situations, a procedure of tomographic analysis of a gas object has been developed. In this procedure, the DL beam is split by optical devices into several beams that cross the region under study along different trajectories in a selected section, and each beam passing through the object is recorded by an individual optical detector. The recording system simultaneously processes the signals of all detectors, yielding the spatial distribution of the required parameters in each engine run. An example of such a system (Fig. 6) shows a DLAS optical circuit, the conditional geometry of the experiment, and the results of determining the temperature in the gas flow exhausting from the turbine of a supersonic engine [23]. In Fig. 6a, the path of the probing beams is indicated by a grid of straight lines. Each beam, passing through the probed region of the exhaust gases, falls on a corresponding photodetector, the signal from which is processed by the data acquisition and processing system. This DLAS procedure results in a more complete picture of processes occurring in the object under study, but it is much more technically complicated, requires a more complex program for processing the results, and is much more expensive. The tomographic procedure is designed to diagnose free gas flows, such as engine exhaust. However, it is not applicable to the diagnostics of closed volumes, such as internal combustion chambers.

Modulation mode of diode laser absorption spectroscopy. So far, we have discussed modes of direct measurements of the intensity of the DL radiation transmitted through the probed region. As already

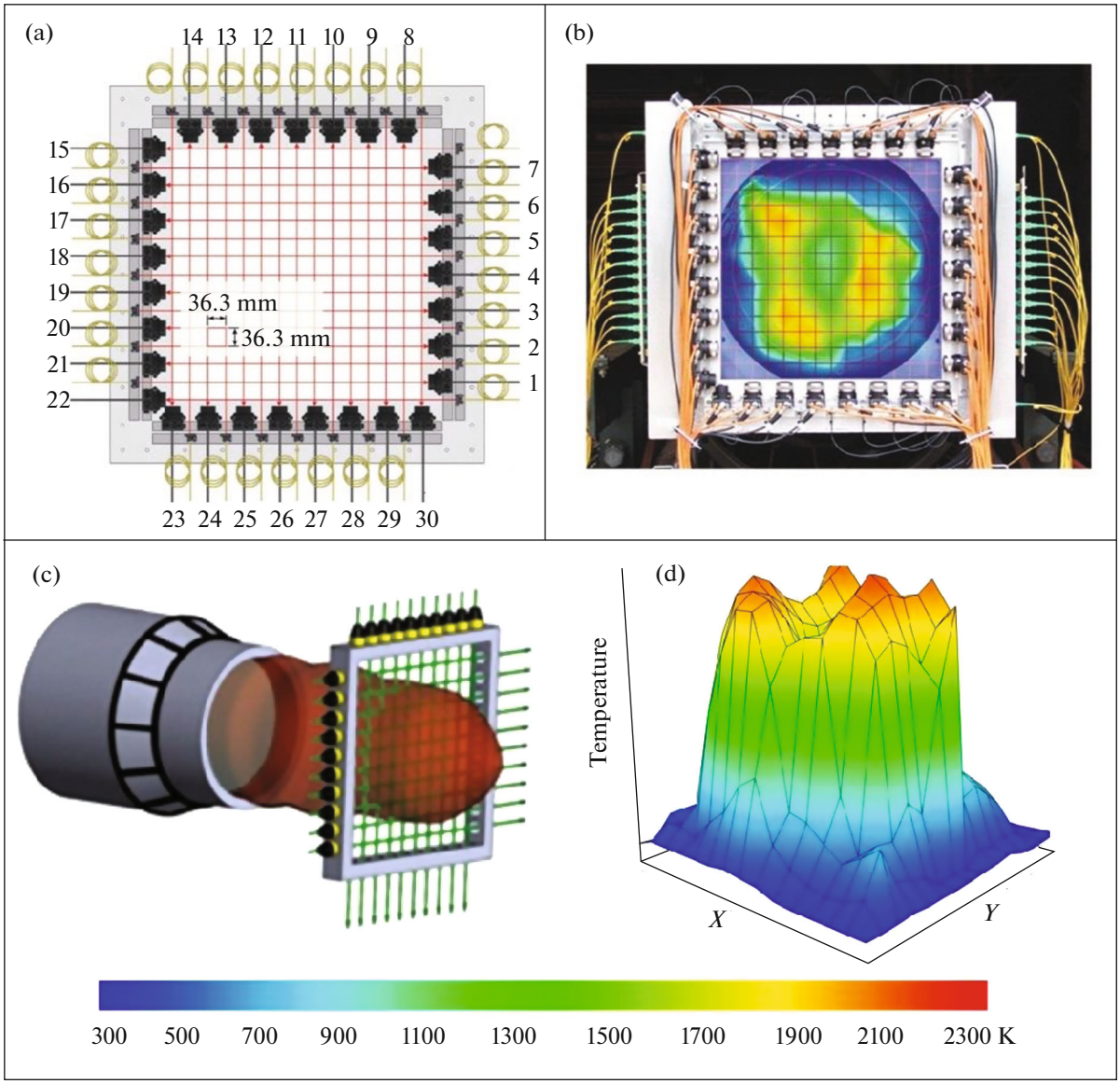

Fig. 6. Tomographic diagnostics of the exhaust gases of an aircraft supersonic engine [23]: (a) the geometry of the probing beams of the diode laser and photodetectors, (b) the view of the real layout of the optical elements, (c) the location of the tomographic device in the exhaust gas jet, and (d) the 3D profile of the temperature distribution in the exhaust gas jet.

noted, such a regime is suitable for relatively strong absorption lines and under the conditions when the magnitude and fluctuations of the background are not too large and the integral intensity of the absorption lines can be determined with sufficient accuracy. The situation becomes more complicated for measurements performed under the conditions of significant electrical and acoustic noise in the object of observation and/or in the recording equipment. For such cases, a version of the DLAS method with the additional modulation of the radiation wavelength has been developed. To do this, a high-frequency current from an additional source is added to the injection current through the laser chip. Thus, in addition to slow scanning of the DL radiation frequency within the spectral region of its tuning at rates of an order of 1 kHz, its wavelength is rapidly modulated with a frequency f of an order of 50–100 kHz. The trick is that the absorption signal is detected at the frequencies that are multiples of the modulation frequency: f, $2f$, ..., nf. In most experimental situations, the main noise is located in the low-frequency region <20–30 kHz; therefore, signal recording at the frequencies above 50 kHz leads to a decrease in the noise level and increases the signal-to-noise ratio. This approach makes it possible to record small absorption signals ($\Delta I/I_0 \le 10^{-5}$–10^{-6}). An example of the effectiveness of such a DLAS version is shown in Fig. 7 [24]: the result of recording absorption lines by the direct detec-

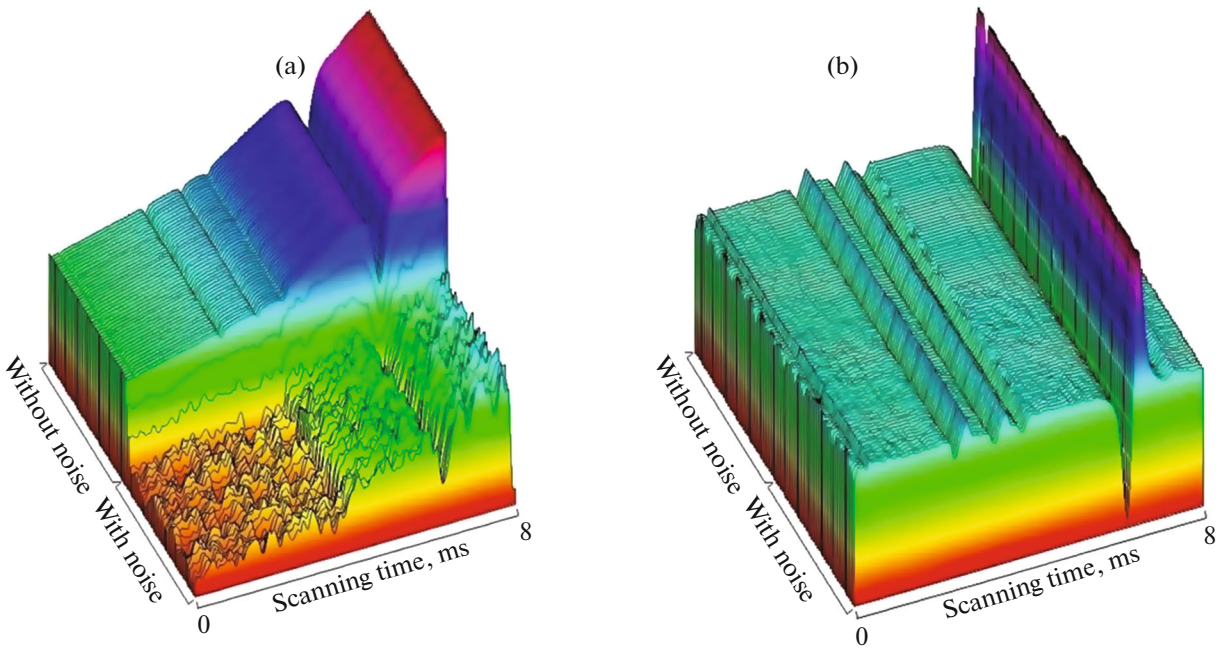

Fig. 7. Effectiveness of the modulation version of DLAS [24]: (a) 3D image of the process diagnosed by the direct absorption recording method and (b) the same process diagnosed by the modulation DLAS method. When excess noise is turned on, the absorption lines completely disappear during direct detection (a) and are reliably recorded by the modulation DLAS method (b).

tion method (Fig. 7a) and the detection of the same lines by the modulation approach (Fig. 7b). The former figure shows confident detection of lines in the absence of excess noise and the complete disappearance of the analytical signal when excess noise is turned on. In the last figure, the absorption lines are reliably detected with a good signal-to-noise ratio even in the presence of excess noise. Note that, in this option of the modulation DLAS, the first derivative of modulation frequency f was recorded.

OTHER APPLICATIONS OF DIODE LASER ABSORPTION SPECTROSCOPY

Diagnostics of internal combustion engines. Direct detection and modulation DLAS techniques have been successfully used in several studies to diagnose working chambers of internal combustion engines (ICEs) [12]. To improve the design of an internal combustion engine, experimental cylinders were created with optical windows for the input and output of the DL probing beam. One such experimental circuit is shown in Fig. 8 [25]. Here, lasers of another type (quantum-cascade lasers) were used, operating in the regions of 4.55 and 4.59 μm, corresponding to the position of strong CO absorption lines. Two diode lasers were used in the experiment; they operated alternately in the pulsed mode. Figure 8b demonstrates the dips in the DL radiation that passed through the probing region at the moment when the DL wavelength coincided with the CO absorption lines. The temperature was determined from the ratio of the integrated absorption intensities for two selected lines. A feature of this DLAS circuit was the detection of absorption at a rather high pressure of the mixture (15–20 atm). At this pressure, the absorption lines broadened significantly. The DL wavelength tunable mode was used, enabling the lasers to be tuned within 2.8 cm^{-1} with frequencies of ~100 kHz.

Control of molecular impurities in the production of gaseous hydrides. A set of equipment and methods for the continuous monitoring of gaseous impurities CO_2, H_2O, CH_4, C_2H_2, C_2H_4, etc. in the process of the low-temperature distillation purification of gaseous hydrides have been developed [26]. High-purity hydrides NH_3, PH_3, AsH_3, SiH_4, and GeH_4 are essential components in manufacturing electronic and optoelectronic products, and the requirements for the purity of the produced hydrides are quite stringent. A change in the impurity composition of hydrides can significantly affect the results of their certification and the quality of the final products. The molecular impurities, analytical lines, and limits of detection for impurities are listed in Table 1.

The instruments were based on diode lasers designed for the near-IR region of 0.7 to 2.0 μm, in which the absorption bands of overtones and composite frequencies of the studied impurities are located. The systems are highly sensitive and rapid in determining the impurity concentration. Because of their compactness and low power consumption, they are easily integrated into the process equipment (in the distillation column units) and enable the continuous

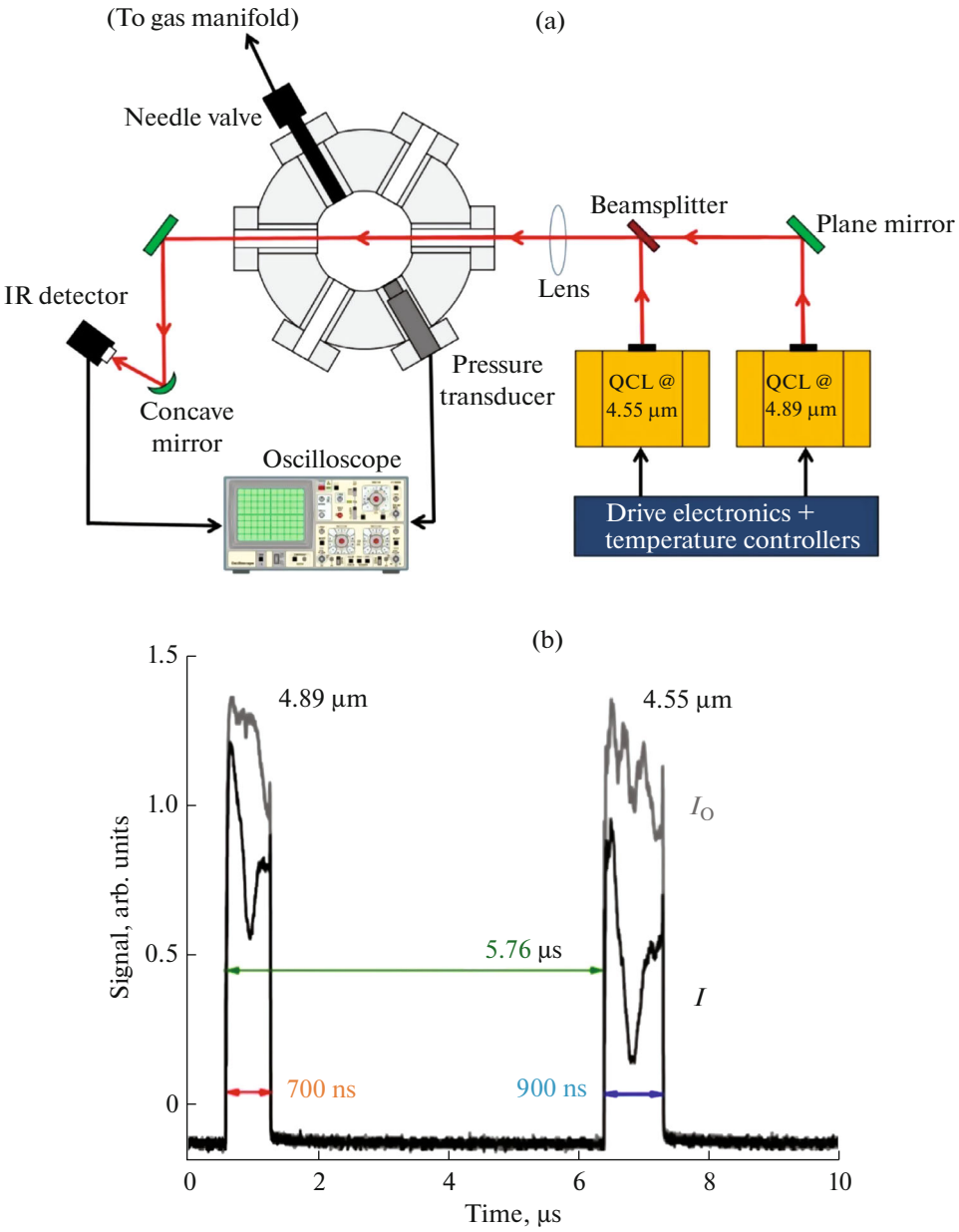

Fig. 8. (a) Monitoring of the combustion process in an internal combustion engine cylinder [25] (QCL, quantum-cascade lasers). (b) Signals recorded by scanning the diode lasers near the absorption lines of CO molecules.

long-term monitoring of the degree of hydride purification.

To achieve high sensitivity, multipass optical cuvettes were used with a fiber input to introduce DL radiation. Cuvettes with a base (geometric) length of 40 cm were developed. Due to the multiple passage of the probing radiation inside the cell, the total optical length of the laser beam reached 25.5 m. As DLAS is used in the vast majority of experiments to determine low concentrations of analytes, the analytical absorption signal depends linearly on the optical path length. A gas mixture under study could be taken and fed into the cuvette at various stages of the rectification process. The cuvette can be positioned in different locations of the distillation column, up to 15 m away from the electronic control unit. New modulation-correlation methods have been developed for the reliable detection of the weak molecular absorption of the impurity being determined against the background of strong selective absorption by the main molecular component of the mixture (the hydride under study).

As an example of the effectiveness of the developed method, let us consider the results of monitoring the purity of ammonia. During rectification, the pressure of the ammonia mixture did not exceed 5 kPa, and the measurement temperature was 23°C. The purity con-

Table 1. Impurities determined using DLAS gas analyzers [26]

Impurity	Detection wavelength, μm	Hydrides	Detection limit, mol %
H_2O	1.391	NH_3, PH_3	1×10^{-4}
NH_3	1.512	AsH_3	5×10^{-5}
C_2H_4	1.635	SiH_4	2×10^{-4}
CH_4	1.651	SiH_4	4×10^{-5}
CO_2	2.004	PH_3, SiH_4, AsH_3	1×10^{-4}
H_2S	1.601	AsH_3	1×10^{-3}
C_2H_2	1.531	PH_3, SiH_4	1×10^{-3}

trol lasted over 1.5 days. According to the DLAS data, the average concentrations of the H_2O impurity in ammonia before and after purification by rectification were 3.0×10^{-3} and 1.0×10^{-5}%, respectively. The results are in good agreement with the data of gas chromatography.

Diagnosis of patient's conditions by an exhaled breath. DLAS is successfully used for medical diagnostics [27]. The works [28, 29] demonstrated a possibility of obtaining objective information about the patient's condition based on the determination of biomarkers $^{12}CO_2$, $^{13}CO_2$, CH_4, H_2S, NH_3, and H_2O in an exhaled breath. A DLAS spectrum analyzer based on three diode lasers, emitting at wavelengths of 1.51, 1.60, and 1.65 μm, has been developed. The diode lasers work simultaneously, ensuring the detection of all biomarkers of interest at once. The air exhaled by a patient entered the cuvette, and the absorption signals of all molecular impurities were recorded simultaneously. To increase the sensitivity and accuracy of the detection of analytes, a multipass Herriot cell with a base of 30 cm and a total optical path length of 26 m was used. The analytical absorption signal increased significantly by increasing the effective length of the optical layer.

Clinical and physiological tests of the device were carried out within a joint project between the Prokhorov General Physics Institute of the Russian Academy of Sciences, the Pirogov Russian State Medical University, and the Buyanov City Clinical Hospital no. 12. The limits of the physiological "norm" and a possible correlation between the deviations from the "norm" and the presence of certain diseases were determined. A histogram in Fig. 9 shows the concentration of ammonia in an exhaled breath in relatively healthy people and patients with peptic ulcers in the phases of remission and exacerbation. The concentration of ammonia in the exhaled breath of a healthy patient is significantly lower than in patients with peptic ulcer for all studied modes (fasting, exercise, rest, food load). Differences in this parameter in patients in remission and exacerbation are also clearly distinguished.

Control of methane leaks on main pipelines. The control of the technical conditions of main pipelines is the key economic and environmental problem. One of methods of such control is a DLAS-based sensor for determining the concentration of methane in the atmosphere near the pipeline. A sensor for detecting methane in the atmosphere, developed at the Prokhorov General Physics Institute of the Russian Academy of Sciences can determine methane concentrations in the range from 200 ppm to 1.7% (lower concentration ignition limit) [30]. The measurements are carried out in a single-pass cuvette vented to the surrounding air. The input and output of the DL radiation from the cell are carried out through an optical fiber, which is fixed at the ends of the cell with the help of special flanges (Fig. 10a). The DLAS-based sensor is mounted on racks installed in places where the pipeline is "punctured" under roads and railways (Fig. 10b). The length of the optical fiber reaches 60 km, which makes it possible to mount sensors on all racks along the pipeline route and collect information on methane concentration at one control unit. More than 60 such sensors were installed in the Anapa South Stream Hub. They control methane leaks in the gas pipeline at the points of intersection with highways and railway lines.

CONCLUSIONS

The review considers the fundamentals of the method of diode laser absorption spectroscopy and presents the most characteristic examples of its application to determining element concentrations and diagnosing processes in hot zones. Tunable diode lasers are unique sources of resonance radiation. The DL wavelength can be tuned with frequencies up to hundreds of megahertz within a few reciprocal centimeters, which makes it possible to record absorption along several selected lines of the analyte over times of an order of 0.1 ms. The width of the DL generation line is 2–3 orders of magnitude smaller than the widths of the absorption lines of free atoms and molecules under typical analytical conditions. Because of this, DL-based sensors do not require the use of bulky

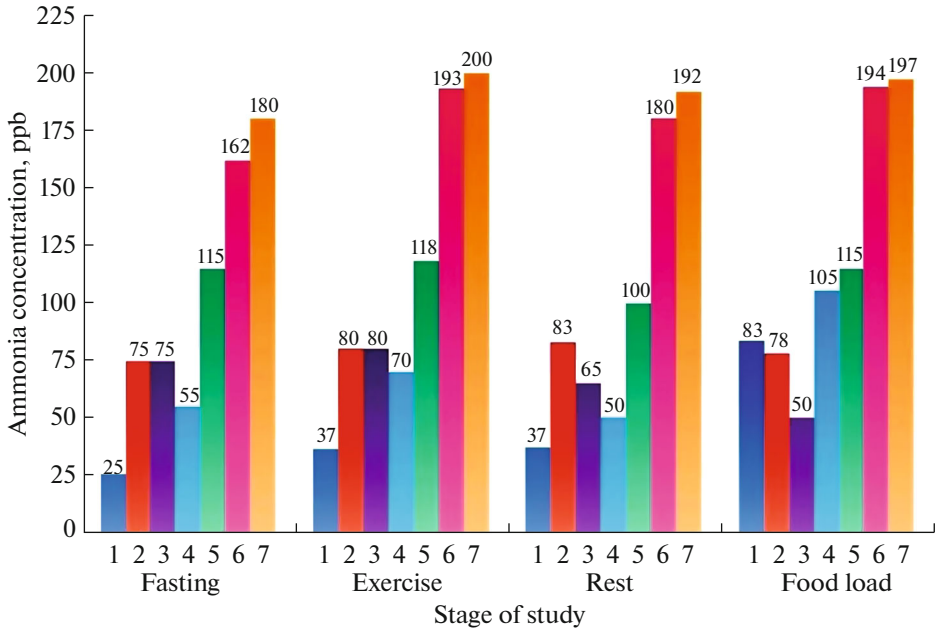

Fig. 9. The concentration of ammonia in the exhaled breath of a healthy patient and patients with peptic ulcer in various regimens and in a state of remission or exacerbation [9, 29]: (*1*) a healthy individual and patients with peptic ulcer (*2–4*) in remission and (*5–7*) in the acute phase. In a healthy patient in all modes, except for the food load, the ammonia concentration is significantly lower than in patients.

or expensive optical spectral devices. These sources are small-sized and controlled by currents of an order of hundreds of milliamperes. They are easily mated with segments of optical fibers, which makes it possible to transmit their radiation hundreds of meters to an object of study without significant power loss.

Diode lasers are used in a variety of analytical and diagnostic applications. The review gives examples of their use for detecting uranium isotopes, molecular impurities in the production of pure hydrides, and a set of molecules in an exhaled breath for the medical diagnosis of patient's conditions. One of the essential tasks solved with the help of DLAS sensors is the control of methane leaks on the main pipelines in Russia, the total length of which exceeds 170000 km.

Remote diagnostics of hot zones, subsonic and supersonic gas flows, and processes in shock tubes are other crucial fields of DLAS application. The DLAS method helps to determine the temperature of an object under study, the total pressure of a gas, and the partial pressures of the molecular components of a gas sample. To determine these parameters, the intensities of two (at least) absorption lines of a test molecule are measured, and temperature is determined under the assumption of a thermodynamic equilibrium in the medium from the ratio of the intensities of lines having different lower transition energy levels. Examples of the diagnostics of combustion zones in mixed flows of fuel and an oxidizer, processes in engine combustion chambers, in gas flows emanating from power units of aircraft engines are also given.

The majority of the works considered in this review were carried out with the simplest diode lasers in the near-IR region. In recent years, more expensive semiconductor lasers have been developed with a wide tuning range and for the spectral region above 3 μm, the so-called quantum cascade lasers. Using quantum cascade lasers, the DLAS method has proven to be effective in detecting a wide range of molecules and radicals in the combustion zone, such as C_nH_m, CO, CO_2, NH, and others [6], as well as for environmental monitoring and the study of atmospheric phenomena [31–33].

FUNDING

The studies were carried out within the framework of the State Program for the Institute of Spectroscopy of the Russian Academy of Sciences. The work was partially supported by the Foundation for Assistance to the Development of Small Forms of Enterprises in the Scientific and Technical Sphere (project no. 270GRNTIS5/42613 dated August 8, 2018) and by the Russian Science Foundation (project no. 19-19-00712 dated 2022).

CONFLICT OF INTEREST

The authors of this work declare that they have no conflicts of interest.

OPEN ACCESS

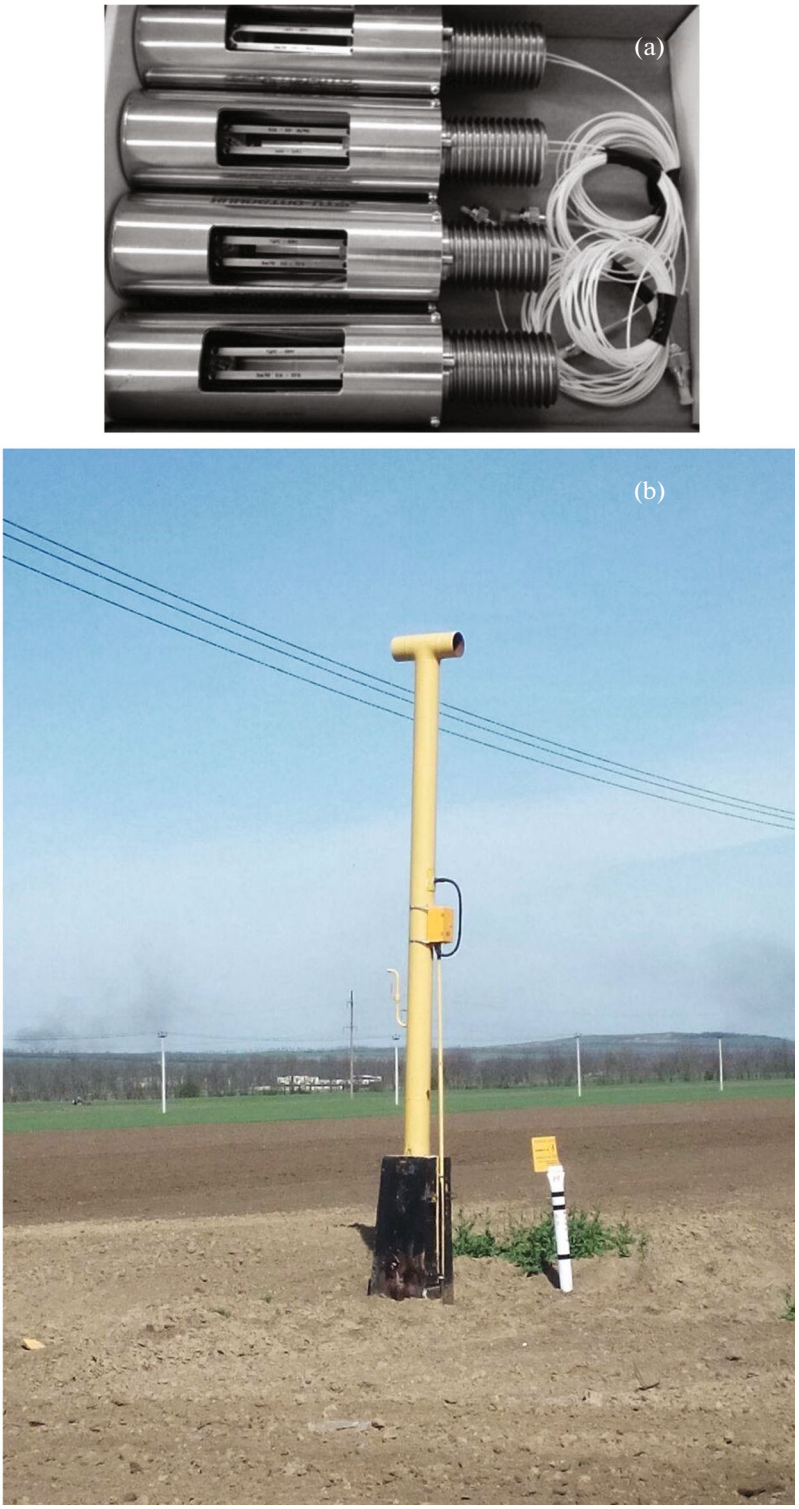

Fig. 10. (a) View of single-pass cuvettes for detecting methane in the atmosphere near a rack located 40 m from the passage of the pipeline through the road or railroad tracks. (b) View of the rack with a DLAS methane detector attached to it. Such racks are installed near each of the 60 intersections of the pipeline with highways.

REFERENCES

1. Imasaka, T., *Talanta*, 1999, vol. 48, no. 2, p. 305. https://doi.org/10.1016/S0039-9140(98)00244-6
2. Landgraf, S., *Spectrochim. Acta, Part A*, 2001, vol. 57, no. 10, p. 2029. https://doi.org/10.1016/S1386-1425(01)00502-9
3. Zeller, W., Naehle, L., Fuchs, P., Gerschuetz, F., Hildebrandt, L., and Koeth, J., *Sensors*, 2010, vol. 10, no. 4, p. 2492. https://doi.org/10.3390/s100402492
4. Li, J., Yu, B., Zhao, W., and Chen, W., *Appl. Spectrosc. Rev.*, 2014, vol. 49, no. 8, p. 666. https://doi.org/10.1080/05704928.2014.903376
5. Bolshov, M.A., Kuritsyn, Yu.A., and Romanovskii, Yu.V., *Spectrochim. Acta, Part B*, 2015, vol. 106, p. 45. https://doi.org/10.1016/j.sab.2015.01.010
6. Goldenstein, C.S., Spearrin, R.M., Jeffries, J.B., and Hanson, R.K., *Prog. Energy Combust. Sci.*, 2017, vol. 60, p. 132. https://doi.org/10.1016/j.pecs.2016.12.002
7. Liu, C. and Xu, L., *Appl. Spectrosc. Rev.*, 2018, vol. 54, no. 1, p. 1. https://doi.org/10.1080/05704928.2018.1448854
8. Liger, V.V., Mironenko, V.R., Kuritsyn, Yu.A., and Bol'shov, M.A., *Opt. Spectrosc.*, 2019, vol. 127, no. 1, p. 49. https://doi.org/10.1134/S0030400X19070166
9. Ponurovskii, Ya.Ya., *Analitika*, 2019, vol. 9, no. 1, p. 68. https://doi.org/10.22184/2227-572x.2019.09.1.68.7
10. Li, J., Yu, Z., Du, Z., Ji, Y., and Liu, C., *Remote Sens.*, 2020, vol. 12, no. 17, p. 2771. https://doi.org/10.3390/rs12172771
11. Fu, B., Zhang, C., Lyu, W., Sun, J., Shang, C., Cheng, Y., and Xu, L., *Appl. Spectrosc. Rev.*, 2022, vol. 57, no. 2, p. 112. https://doi.org/10.1080/05704928.2020.1857258
12. Farooq, A., Alquaity, A.B.S., Raza, M., Nasir, E.F., Yao, S., and Ren, W., *Prog. Energy Combust. Sci.*, 2022, vol. 91, p. 100997. https://doi.org/10.1016/j.pecs.2022.100997
13. Smith, B.W., Quentmeier, A., Bolshov, M., and Niemax, K., *Spectrochim. Acta, Part B*, 1999, vol. 54, no. 6, p. 943. https://doi.org/10.1016/S0584-8547(99)00022-1
14. Quentmeier, A., Bolshov, M., and Niemax, K., *Spectrochim. Acta, Part B*, 2001, vol. 56, no. 1, p. 45. https://doi.org/10.1016/S0584-8547(00)00289-5
15. Li, F., Yu, X., Cai, W., and Ma, L., *Appl. Opt.*, 2012, vol. 51, no. 20, p. 4788. https://doi.org/10.1364/AO.51.004788
16. Zybin, A., Schnurer-Patschan, C., Bolshov, M., and Niemax, K., *TrAC, Trends Anal. Chem.*, 1998, vol. 17, p. 513. https://doi.org/10.1016/S0165-9936(98)00063-6
17. Bolshov, M.A., Kuritsyn, Yu.A., Liger, V.V., Mironenko, V.R., Leonov, S.B., and Yarantsev, D.A., *Quantum Electron.*, 2009, vol. 39, no. 9, p. 869. https://doi.org/10.1070/QE2009v039n09ABEH014044
18. Bol'shov, M.A., Kuritsyn, Yu.A., Leonov, S.B., Liger, V.V., Mironenko, V.R., Savelkin, K.V., and Yarantsev, D.A., *Teplofiz. Vys. Temp.*, 2010, no. 1 (suppl.), p. 9.
19. Bolshov, M.A., Kuritsyn, Yu.A., Liger, V.V., Mironenko, V.R., Leonov, S.B., and Yarantsev, D.A., *Appl. Phys. B*, 2010, vol. 100, no. 2, p. 397. https://doi.org/10.1007/s00340-009-3882-4
20. Gordon, I.E., Rothman, L.S., Hargreaves, R.J., Hashemi, R., Karlovets, E.V., et al., *J. Quant. Spectrosc. Radiat. Transfer*, 2022, vol. 277, p. 107949. https://doi.org/10.1016/j.jqsrt.2021.107949
21. Bol'shov, M.A., Kuritsyn, Yu.A., Liger, V.V., Mironenko, V.R., and Kolesnikov, O.M., *Opt. Spectrosc.*, 2017, vol. 122, no. 5, p. 705.
22. Liger, V.V., Kuritsyn, Yu.A., Mironenko, V.R., Bol'shov, M.A., Ponurovskii, Ya.Ya., and Kolesnikov, O.M., *High Temp.*, 2018, vol. 56, no. 1, p. 98. https://doi.org/10.1134/S0018151X18010108
23. Ma, L., Li, X., Sanders, S.T., Caswell, A.W., Roy, S., Plemmons, D.H., and Gord, J.R., *Opt. Express*, 2013, vol. 21, no. 1, p. 1152. https://doi.org/10.1364/OE.21.001152
24. Liger, V.V., Mironenko, V.R., Kuritsyn, Yu.A., and Bolshov, M.A., *Sensors*, 2023, vol. 23, no. 2, p. 622. https://doi.org/10.3390/s23020622
25. Nasir, E.F. and Farooq, A., *Proc. Combust. Inst.*, 2017, vol. 36, p. 4453. https://doi.org/10.1016/j.proci.2016.07.010
26. Ponurovskii, Ya.Ya., Stavrovskii, D.B., Shapovalov, Yu.P., Spiridonov, M.V., Kuz'michev, A.S., Nadezhdinskii, A.I., Kotkov, A.P., Grishnova, N.D., Anoshin, O.S., Skosyrev, A.I., and Polezhaev, D.M., *Inorg. Mater.*, 2020, vol. 56, p. 1284. https://doi.org/10.1134/S0020168520120158
27. Wang, C. and Sahay, P., *Sensors*, 2009, vol. 9, no. 10, p. 8230. https://doi.org/10.3390/s91008230
28. Ponurovsky, Ya.Ya., Nadezhdinsky, A.I., Stavrovsky, D.B., Shapovalov, Yu.P., Spiridonov, M.V., Kuzmichev, A.S., Karabinenko, A.A., and Petrenko, Yu.M., *Sovrem. Tehnol. Med.*, 2020, vol. 12, no. 5, p. 71. https://doi.org/10.17691/stm2020.12.5.08
29. Karabinenko, A.A., Nadezhdinsky, A.I., Ponurovsky, Ya.Ya., Presnova, E.D., and Nikitin, I.G., *Wschodnioeur. Czas. Nauk.*, 2018, vol. 29, no. 1, p. 30.
30. Pleshkov, D.I., Kulakov, A.T., Ponurovskii, Ya.Ya., Shapovalov, Yu.P., and Nadezhdinskii, A.I., RF Patent 2598694, 2016.
31. Risby, T.H. and Tittel, F.K., *Opt. Eng.*, 2010, vol. 49, no. 11, p. 111123. https://doi.org/10.1117/1.3498768
32. Li, J.S., Chen, W., and Fischer, H., *Appl. Spectrosc. Rev.*, 2013, vol. 48, no. 7, p. 523. https://doi.org/10.1080/05704928.2012.757232
33. Du, Z., Zhang, S., Li, J., Gao, N., and Tong, K., *Appl. Sci.*, 2019, vol. 9, no. 2, p. 338. https://doi.org/10.3390/app9020338

Translated by O. Zhukova